Freezing and collapse of flexible polymers on regular lattices in three dimensions

Thomas Vogel,[1,*] Michael Bachmann,[1,2,†] and Wolfhard Janke[1,‡]

[1]*Institut für Theoretische Physik, Universität Leipzig, Postfach 100 920, D-04009 Leipzig, Germany*
and Centre for Theoretical Sciences (NTZ), Emil-Fuchs-Straße 1, D-04105 Leipzig, Germany
[2]*Computational Biology and Biological Physics Group, Department of Theoretical Physics,*
Lund University, Sölvegatan 14A, SE-223 62 Lund, Sweden

We analyze the crystallization and collapse transition of a simple model for flexible polymer chains on simple-cubic and face-centered-cubic lattices by means of sophisticated chain-growth methods. In contrast to the bond-fluctuation polymer model in certain parameter ranges, where these two conformational transitions were found to merge in the thermodynamic limit, we conclude from our results that the two transitions remain well separated in the limit of infinite chain lengths. The reason for this qualitatively distinct behavior is presumably due to the ultrashort attractive interaction range in the lattice models considered here.

PACS number(s): 36.20.Ey, 05.10.−a, 87.15.Aa, 87.15.Cc

I. INTRODUCTION

The analysis of conformational transitions that a single polymer in solvent can experience is surprisingly difficult. In good solvent (or high temperatures), solvent molecules occupy binding sites of the polymer and, therefore, the probability of noncovalent bonds between attractive segments of the polymer is small. The dominating structures in this phase are dissolved or random coils. Approaching the critical point at the Θ temperature, the polymer collapses and in a cooperative arrangement of the monomers, globular conformations are favorably formed. At the Θ point, which has already been studied over many decades, the infinitely long polymer behaves like a Gaussian chain, i.e., the effective repulsion due to the volume exclusion constraint is exactly balanced by the attractive monomer-monomer interaction. Below the Θ temperature, the polymer enters the globular phase, where the influence of the solvent is small. Globules are very compact conformations, but there is little internal structure, i.e., the globular phase is still entropy-dominated. For this reason, a further transition toward low-degenerate energetic states is expected to happen: the freezing or crystallization of the polymer. Since this transition can be considered as a liquid-solid phase separation process, it is expected to be of first order, in contrast to the Θ transition, which exhibits characteristics of a second-order phase transition [1,2].

The complexity of this problem appears in the quantitative description of these processes. From the analysis of the corresponding field theory [3] it is known that the Θ transition is a tricritical point with upper critical dimension $d_c = 3$, i.e., multiplicative and additive logarithmic corrections to the Gaussian scaling are expected and, indeed, predicted by field theory [4–7]. However, until now neither experiments nor computer simulations could convincingly provide evidence for these logarithmic corrections. This not only regards analyses of different single-polymer models [8–14], but also the related problem of critical mixing and unmixing in polymer solutions [15–19].

In a remarkable recent study of a bond-fluctuation polymer model, it was shown that, depending on the intramolecular interaction range, collapse and freezing transition can fall together in the thermodynamic limit [12,13]. This surprising phenomenon is, however, not general. For an off-lattice bead-spring polymer with finitely extensible nonlinear elastic (FENE) bond potential and intramonomer Lennard-Jones interaction, for example, it could be shown that both transitions remain well separated in the limit of infinitely long chains [14].

In our study, we investigate collapse and freezing of a single homopolymer restricted to simple-cubic (sc) and face-centered-cubic (fcc) lattices. We primarily focus on the freezing transition, where comparatively little is known as most of the analytical and computational studies in the past were devoted to the controversially discussed collapse transition; see, e.g., Refs. [8,11,16–18,20–26]. A precise statistical analysis of the conformational space relevant in this low-temperature transition regime is difficult as it is widely dominated by highly compact low-energy conformations which are entropically suppressed. Most promising for these studies appear sophisticated chain-growth methods based on Rosenbluth sampling [27] combined with improved pruning-enrichment strategies [11,28] which, in their original formulation, are particularly useful for the sampling in the Θ regime. For the analysis of the freezing transition, we apply in our simulations generalized-ensemble contact-density variants [29,30], which have proven to be very successful in the low-energy sampling of proteinlike heteropolymers [29] and the adsorption of polymers and peptides to solid substrates [31,32]. The precision of these algorithms when applied to lattice polymers as in the present study, is manifested by unraveling even finite-length effects induced by symmetries of the underlying lattice.

The rest of the paper is organized as follows. In Sec. II, the lattice model for flexible polymers and the employed chain-growth methods, which allow for a precise statistical sampling even in the low-temperature regime, are described.

*thomas.vogel@itp.uni-leipzig.de
†michael.bachmann@itp.uni-leipzig.de
‡wolfhard.janke@itp.uni-leipzig.de;
http://www.physik.uni-leipzig.de/CQT.html

The conformational transitions the polymers experience on sc and fcc lattices are discussed in Sec. III. Here, we also present our results for the scaling of the collapse transition temperature in comparison with various approaches known from the literature. Eventually, in Sec. IV, the paper is concluded by a summary of our findings.

II. MODEL AND METHODS

For our studies, we employ the interacting self-avoiding walk (ISAW) model for lattice polymers. In this model, the polymer chain is not allowed to cross itself, i.e., a lattice site can only be occupied by a single monomer. In order to mimic the "poor solvent" behavior in the energetic regime, i.e., at low temperatures, nearest-neighbor contacts of nonadjacent monomers reduce the energy. Thus, the most compact conformations possess the lowest energy. Formally, the total energy of a conformation $\mathbf{X}=\{\mathbf{x}_1,\mathbf{x}_2,\ldots,\mathbf{x}_N\}$ of a chain with N beads is simply given as

$$E(\mathbf{X}) = -\varepsilon_0 n_{\mathrm{NN}}(\mathbf{X}), \qquad (1)$$

where ε_0 is an unimportant energy scale (which is set $\varepsilon_0 \equiv 1$ in the following) and $n_{\mathrm{NN}}(\mathbf{X})$ is the number of nearest-neighbor contacts between nonbonded monomers.

The total number of self-avoiding lattice conformations with $m=N-1$ bonds scales as [33,34]

$$C_m \sim \mu^m m^{\gamma-1}, \qquad (2)$$

where μ is the effective coordination number of the lattice and $\gamma \approx 1.16$ is a universal exponent. For the sc lattice, the connectivity constant is $\mu_{\mathrm{sc}} \approx 4.684$ and in the fcc case $\mu_{\mathrm{fcc}} \approx 10.036$ [35–41]. Due to this exponential growth of the number of conformations, the investigation of all conformational transitions a homopolymer of a given length can experience requires employing numerical methods being capable of estimating the density of states for all possible energies with high precision. There exist mainly two strategies for generating and updating conformations within the stochastic search schemes typically used. Applying standard Markov chain Monte Carlo methods, conformational updates include semilocal changes of bond orientations as, among others, corner and end flips, crankshaft moves, and more nonlocal updates such as pivot rotations. In our work, we have used the alternative concept of chain growth. Depending on the lattice constraints, a new monomer is tried to be attached to an end of the already existing chain until the total length or a "dead end" is reached, i.e., all neighbors are already occupied and, thus, the chain end is trapped. In an early approach, the Rosenbluth method [27], first the number of free nearest neighbors k for the possible placements of the lth monomer is determined. Then, one of the possibilities (if any) is selected randomly. The peculiarity is that this algorithm introduces a bias as the (athermal) probability of generating a certain chain conformation $\mathbf{X}$ of length N, $p(\mathbf{X}) = \prod_{l=2}^{N} k_l^{-1}$, depends on the growth direction. Thus, identical walks can possess different construction probabilities, if they, e.g., were grown "forward" or "backward." For correct statistics, this bias must be corrected by introducing Rosen-

bluth weights $w(\mathbf{X})=p^{-1}(\mathbf{X})$. Actually, this bias can be utilized to increase the efficiency of the method in generating self-avoiding walks which is particularly useful for the ISAW model of lattice polymers. For this purpose it is convenient to introduce for each chain a thermal Rosenbluth weight $W(\mathbf{X})=\prod_{l=2}^{N} k_l \exp\{-[E(\mathbf{x}_l)-E(\mathbf{x}_{l-1})]/k_B T\}$ (where k_B is the Boltzmann constant which we set to $k_B \equiv 1$ in our analysis). Since this method is a clever kind of simple sampling, the partition sum can be estimated *absolutely* as $Z_N \approx \sum_{i=1}^{I_N} W(\mathbf{X}_i)/M$, where I_N is the number of successfully generated polymer chains of length N in M growth starts [11]. In principle, since $Z_N = \sum_E g_N(E)\exp(-E/k_B T)$, an absolute estimate of the density of states $g_N(E)$, i.e., the degeneracy of energetic states E, is then also known. This is particularly important for heteropolymers, where the ground-state degeneracy is considered as a measure for the stability of native folds of lattice proteins [29]. An essential improvement of the efficiency of this chain-growth approach was reached by the introduction of the pruned-enriched Rosenbluth method (PERM) [11] and its enhanced variants [28], which combine Rosenbluth chain growth with a "Go with the Winners" [42] strategy. In these algorithms, at each stage of the growth process copies of the already existing chain segment are created and continue growing independently, if the accumulated Rosenbluth weight is larger than an upper threshold. If the weight falls below a lower bound, the chain is pruned with a certain probability (which is typically chosen 1/2). Otherwise, the growth of the single chain simply continues. This method has frequently been applied in studies of the Θ point [8,11,16,26]. In our study, we use the nPERMss (new PERM with simple sampling) variant [28] for the simulation of Θ polymers with chain lengths of up to 32 000 (sc) and 4000 (fcc) monomers, respectively.

For the analysis of the conformational behavior below the Θ point, we use even more sophisticated, generalized-ensemble variants which are independent of the temperature and yield an improved estimate for the density of states $g(E)$ within a single simulation. These algorithms combine PERM-based chain growth with multicanonical [29] or flat-histogram techniques [30] and increase, in particular, the sampling of entropically suppressed ("rare") conformations, which are, for example, essential for the study of the freezing transition. Due to the much higher demands in this regime, maximum chain lengths, for which precise results were reliably obtained, are $N=125$ (sc) and 56 (fcc), respectively.

For our statistical analysis, it is convenient to define energetic statistical expectation values via the density of states, i.e., $\langle O(E) \rangle = \sum_E g_N(E) O(E) \exp(-E/k_B T)/Z_N$. The main results of our analysis are based on the peak structure of the specific heat which is defined as $C_V(T) = d\langle E \rangle / dT = (\langle E^2 \rangle - \langle E \rangle^2)/k_B T^2$.

III. RESULTS AND DISCUSSION

It was recently found for a bond-fluctuation model with intermonomeric interaction radius $r=\sqrt{6}$ that in the infinite chain-length limit collapse and freezing are indistinguishable phase transitions appearing at the same temperature (the Θ

temperature T_Θ) [12,13]. In a bead-spring FENE model analysis [14], this phenomenon could not be observed: Both transitions exist in the thermodynamic limit and the crossover peaks in the specific heat remain well separated. The same observation was made independently in Ref. [13] for the bond-fluctuation model with increased interaction range. In the following, we perform for the lattice polymer model (1) a detailed analysis of these transitions on regular sc and fcc lattices and discuss the expected behavior in the thermodynamic limit.

A. The expected peak structure of the specific heat

Statistical fluctuations of the energy, as expressed by the specific heat, can signalize thermodynamic activity. Peaks of the specific heat as a function of temperature are indicators for transitions or crossovers between physically different macrostates of the system. In the thermodynamic limit, the collective activity, which influences typically most of the system particles, corresponds to thermodynamic phase transitions. For a flexible polymer, three main phases are expected: The random-coil phase for temperatures $T > T_\Theta$, where conformations are unstructured and dissolved; the globular phase in the temperature interval $T_m < T < T_\Theta$ (T_m, melting temperature) with condensed, but unstructured ("liquid") conformations dominating; and for $T < T_m$ the "solid" phase characterized by locally crystalline or amorphous metastable structures. In computer simulations, only polymers of finite length are accessible and, therefore, the specific heat possesses typically a less pronounced peak structure, as finite-length effects can induce additional signals of structural activity and shift the transition temperatures. These effects, which are typically connected with surface-reducing monomer rearrangements, are even amplified by steric constraints in lattice models as used in our study. Although these pseudotransitions are undesired in the analysis of the thermodynamic transitions, their importance in realistic systems is currently increasing with the high-resolution equipment available in experiment and technology. The miniaturization of electronic circuits on polymer basis and possible nanosensory applications in biomedicine will, therefore, require a more emphasized analysis of the finite-length effects in the future.

B. Simple-cubic lattice polymers

Figure 1 shows typical examples of specific heats for very short chains on the sc lattice and documents the difficulty of identifying the phase structure of flexible homopolymers. The 27-mer exhibits only a single dominating peak—which is actually only an sc lattice effect. The reason is that the ground states are cubic ($3 \times 3 \times 3$) and the energy gap toward the first excited states is $\Delta E = 2$ [43]. Actually, also the most pronounced peaks for $N = 48$ ($4 \times 4 \times 3$) and $N = 64$ ($4 \times 4 \times 4$) are due to the excitation of perfectly cuboid and cubic ground states, respectively. The first significant onset of the collapse transition is seen for the 48-mer close to $T \approx 1.4$. A clear discrimination between the excitation and the melting transition is virtually impossible. In these ex-
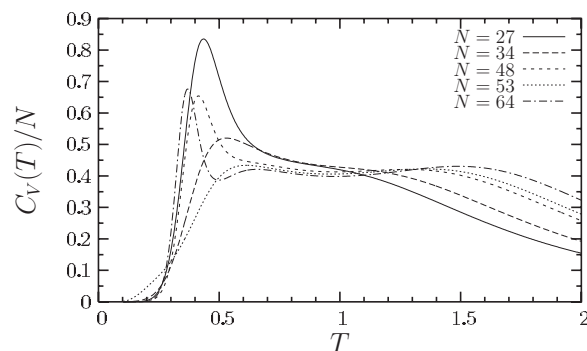

FIG. 1. Examples of specific-heat curves (per monomer) for a few exemplified short homopolymers on the sc lattice. Absolute errors (not shown) are smaller than 0.03 in the vicinity of the low-temperature peaks and smaller than 10^{-5} in the onset of the Θ-transition region near $T \approx 1.5$.

amples, solely for $N = 64$ three separate peaks are present. The plots in Figs. 2(a)–2(c) show representative conformations in the different pseudophases of the 64-mer. Due to the energy gap, the excitations of the cubic ground state with energy $E = -81$ (not shown) to conformations with $E = -79$ [Fig. 2(a)] result in a pseudotransition which is represented by the first specific-heat peak in Fig. 1. The second less-pronounced peak in Fig. 1 around $T \approx 0.6$–0.7 signalizes the melting into globular structures, whereas at still higher temperatures $T \approx 1.5$ the well-known collapse peak indicates the dissolution into the random-coil phase.

The distribution of the maximum values of the specific heat C_V^{max} with respect to the maximum temperatures $T_{C_V^{max}}$ is shown in Fig. 3. Not surprisingly, the peaks belonging to the
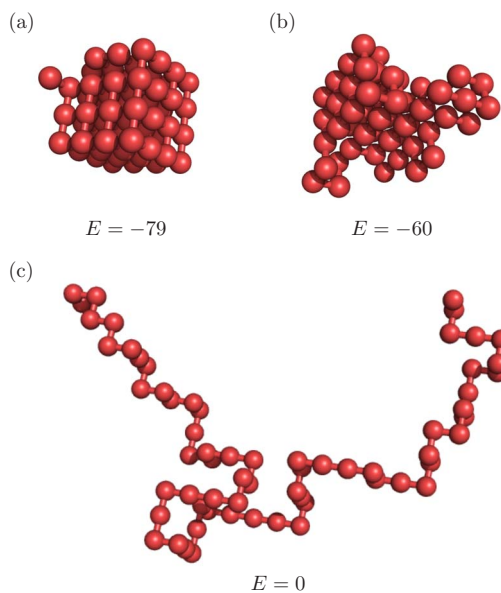

FIG. 2. (Color online) Representative conformations of a 64-mer in the different pseudophases: (a) Excitation from the perfect $4 \times 4 \times 4$ cubic ground state (not shown, $E = -81$) to the first excited crystal state, (b) transition toward globular states, and (c) dissolution into random-coil conformations.
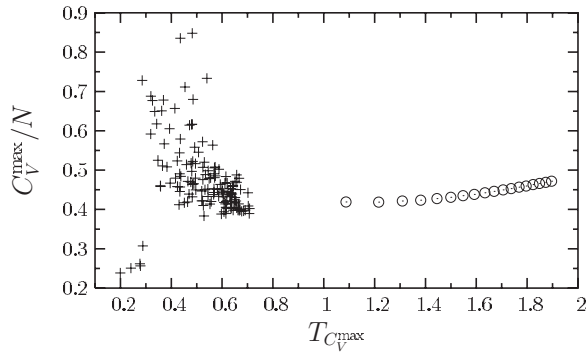
FIG. 3. Map of specific-heat maxima for several chain lengths taken from the interval $N \in [8, 125]$. Circles ($\odot$) symbolize the peaks (if any) identified as signals of the collapse ($T_{C_V^{\max}} > 1$). The low-temperature peaks (+) belong to the excitation-freezing transitions ($T_{C_V^{\max}} < 0.8$). The group of points in the lower left-hand corner correspond to polymers with $N_c + 1$ monomers, where N_c denotes the "magic" lengths allowing for cubic or cuboid ground-state conformations (see Fig. 4 and text).

excitation and freezing transitions (+) appear to be irregularly "scattered" in the low-temperature interval $0 < T_{C_V^{\max}} < 0.8$. The height of the peaks indicating the collapse transition of the finite-length polymers ($\odot$) is, on the other hand, monotonously increasing with the collapse-peak temperature.

Figures 4(a) and 4(b), showing the respective chain-length dependence of the maximum temperatures and maximum specific-heat values, reveal a more systematic picture. At least from the results for the short chains shown, general scaling properties for the freezing transition cannot be read off at all. The reason is that the low-temperature behavior of these short chains is widely governed by lattice effects. This is clearly seen by the "sawtooth" segments. Whenever the sc chain possesses a "magic" length N_c such that the ground state is cubic or cuboid (i.e., $N_c \in \mathcal{N}_c = \{8, 12, 18, 27, 36, 48, 64, 80, 100, 125, \ldots\}$), the energy gap $\Delta E = 2$ between the ground-state conformation and the first excited state entails a virtual energetic barrier which results in an excitation transition. Since entropy is less relevant in this regime, this energetic effect is not "averaged out" and, therefore, causes a pronounced peak in the specific heat [see Fig. 4(b)] at comparatively low temperatures [Fig. 4(a)]. This peculiar sc lattice effect vanishes widely by increasing the length by unity, i.e., for chain lengths $N_c + 1$. In this case, the excitation peak either vanishes or remains as a remnant of less thermodynamic significance. The latter appears particularly in those cases, where $N = N_c + 1$ with $N_c = L^3$ (with L being any positive integer) is a chain length allowing for perfectly cubic ground states. Increasing the polymer length further, the freezing peak dominates at low temperatures. Its peak increases with the chain length, whereas the peak temperature decreases. Actually, with increasing chain length, the character of the transition converts from freezing to excitation, i.e., the entropic freedom that still accompanies the melting-freezing process decreases with increasing chain length. In other words, cooperativity is lost: only a small fraction of
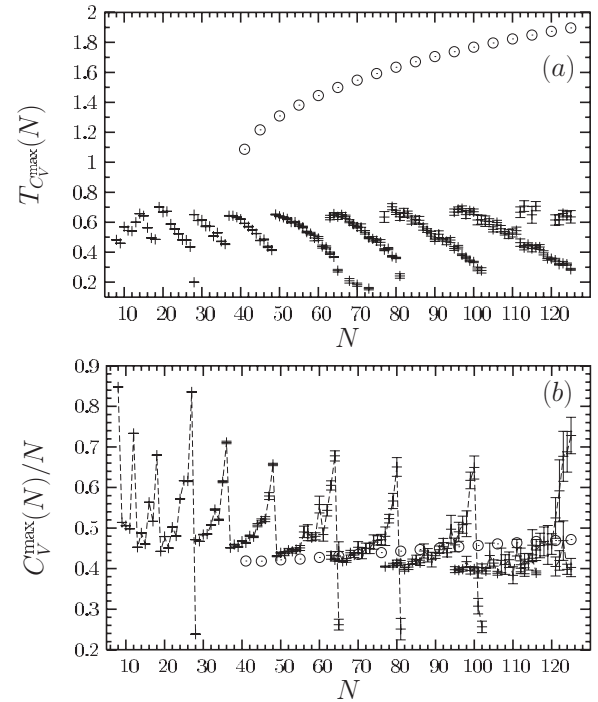

FIG. 4. (a) Collapse ($\odot$) and crystallization-excitation (+) peak temperatures of the specific heat for all chain lengths in the interval $N \in [8, 125]$. (b) Values of the specific-heat maxima in the same interval. Error bars for the collapse transition data (not shown) are much smaller than the symbol size. Θ peaks appear starting from $N = 41$. For the sake of clarity, not all intermediate Θ data points are shown (only for $N = 41, 45, 50, \ldots$).

monomers—residing in the surface hull—is entropically sufficiently flexible to compete the energetic gain of highly compact conformations. This flexibility is reduced the more, the closer the chain length N approaches a number in the "magic" set $\mathcal{N}_c$. If the next length belonging to $\mathcal{N}_c$ is reached, the next discontinuity in the monotonic behavior occurs. Since noticeable "jumps" are only present for chain lengths whose ground states are close to cubes ($N_c = L^3$) or cuboids with $N_c = L^2(L \pm 1)$, the length of the branches in between scales with $\Delta N_c \sim L^2 \sim N_c^{2/3}$. Therefore, only for very long chains on the sc lattice, for which, however, a precise analysis of the low-temperature behavior is extremely difficult, a reasonable scaling analysis for $T_{C_V^{\max}}(N)$ and $C_V^{\max}(N)$ could be performed.

Exemplified for chains of lengths $N = N_c - 1$, N_c, and $N_c + 1$ with $N_c = 36, 64$, specific heats and densities of states are shown in Figs. 5(a)–5(d), which exhibit the length-dependent characteristic properties discussed above. While in Fig. 5(a) for chain lengths around $N = 36$ only some low-temperature activity is visible and the collapse transition is vaguely indicated by a broad shoulder, the transition characteristics are better resolved for $N = 64$ shown in Fig. 5(c). The most pronounced low-temperature peak of the specific heat of the 64-mer, for example, is the excitation peak, the second peak belongs to the freezing transition, and the third, still very shallow peak signals the collapse transition. The low-temperature behaviors of the 63-mer and the 65-mer are
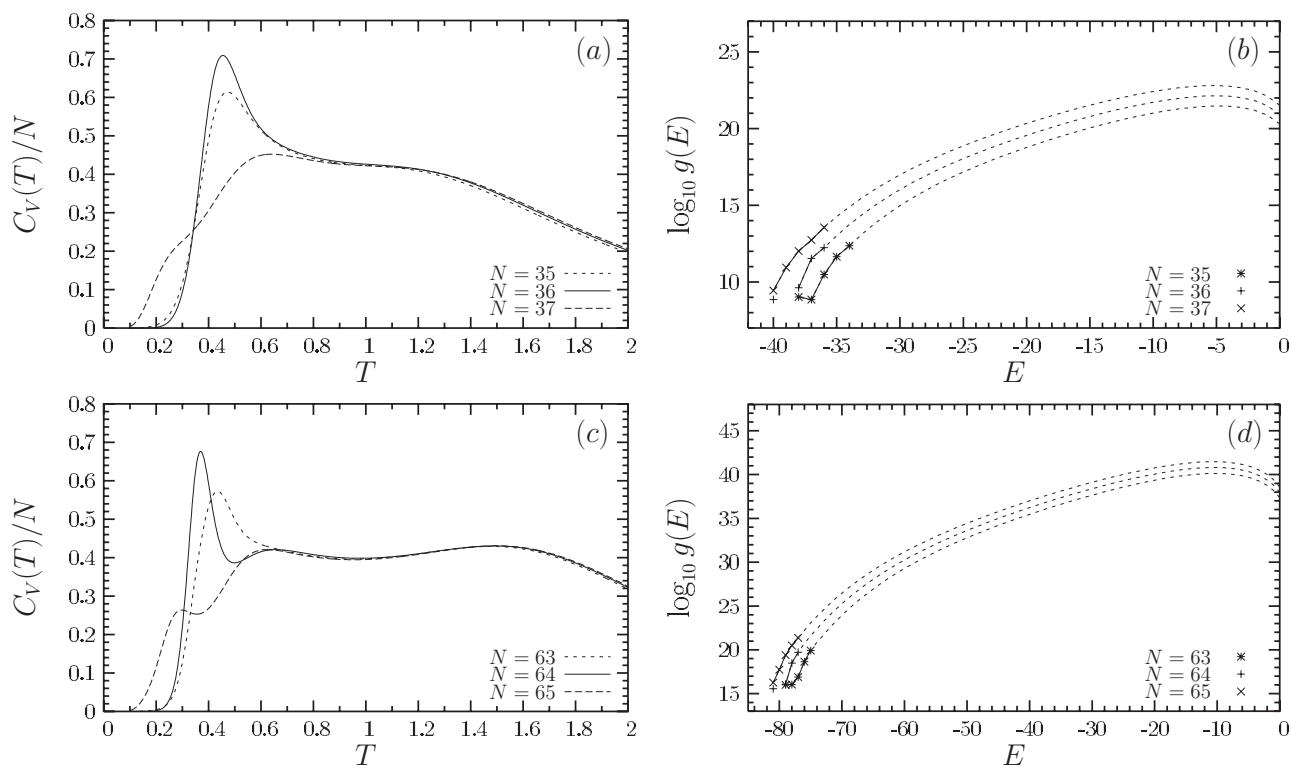
FIG. 5. Examples of specific heats for polymers with (a) $N_c = 4 \times 3 \times 3 = 36$ and $N_c \pm 1$ and (c) $N_c = 4 \times 4 \times 4 = 64$ and $N_c \pm 1$ monomers. In (b) and (d), the respective densities of states are shown (lines are only guides to the eye). Symbols $*$, $+$, and $\times$ emphasize the lowest-energy states. Note the energy gaps between the ground and the first excited states in the compact cases $N_c = 36, 64$ and the dip for $N = 35, 63$.

quite different: While the low-temperature peak of the 63-mer close to $T \approx 0.4$ is due to excitation as is indicated by the $E = -79$ "dip" in the density of states in Fig. 5(d) [similar to the 35-mer in Fig. 5(b) at $E = -38$], the relevant peak for the 65-mer is the freezing peak close to $T \approx 0.6$. In this case, the excitation is of much less relevance (although it is still reflected by a small peak near $T \approx 0.3$). This is a consequence of the missing convex lowest-energy dip in the density of states (or microcanonical entropy). The convex monotony is a signal of a strong first-order phase separation [44,45]. This is confirmed by analyzing the canonical energy distributions for the examples $N = N_c - 1$, N_c, and $N_c + 1$ with $N_c = 36, 64$ shown in Figs. 6(a)–6(c) for temperatures close to the respective excitation and freezing transitions. For $N_c - 1 = 35, 63$ [Fig. 6(a)], the pronounced excitation transition is expressed by the respective double peaks with the strong gap in between, which are for the polymers with chain lengths $N_c = 36, 64$ [Fig. 6(b)] due to the energy gap between ground state and first excited state. This induces the first-order-like character of this pseudotransition. The energy distributions for various temperatures shown in Fig. 6(c) for the case $N = N_c + 1 = 65$ do not exhibit, on the other hand, pronounced double-peaked shapes. The excitation transition at extremely low energies is still weakly present as a small shoulder in the distribution at the corresponding temperature. The freezing transition is associated with slightly larger energies (and temperature) and visible in the distribution with a weak tendency to a double-peaked shape.

The collapse transitions of the finite-length polymers are not affected by the intricate low-energy conformations on the

sc lattice and exhibit a continuous monotony. This will be analyzed in Sec. III D in more detail.

C. Polymers on the fcc lattice

The general behavior of polymers on the fcc lattice is comparable to what we found for the sc polymers. The main difference is that excitations play only a minor role, and the freezing transition dominates the conformational behavior of the fcc polymers at low temperatures. Nonetheless, finite-length effects are still apparent as can be seen in the chain-length dependence of the peak temperatures and peak values of the specific heats plotted in Fig. 7(a) and Fig. 7(b), respectively. Figure 7(a) shows that the locations of the freezing and collapse transitions clearly deviate with increasing chain lengths and we hence can conclude that also for fcc polymers there is no obvious indication that freezing and collapse could fall together in the thermodynamic limit.

Similar to the sc polymers, the finite-length effects at very low temperatures are apparently caused by the usual compromise between maximum compactness, i.e., maximum number of energetic (nearest-neighbor) contacts, and steric constraints of the underlying rigid lattice. The effects are smaller than in the case of the sc lattice, as there are no obvious "magic" topologies in the fcc case. Ground-state conformations for a few small polymers on the fcc lattice are shown in Fig. 8. The general tendency is that the lowest-energy conformations consist of layers of net planes with (111) orientation, i.e., the layers themselves possess triangular pattern with side lengths equal to the fcc nearest-neighbor distance
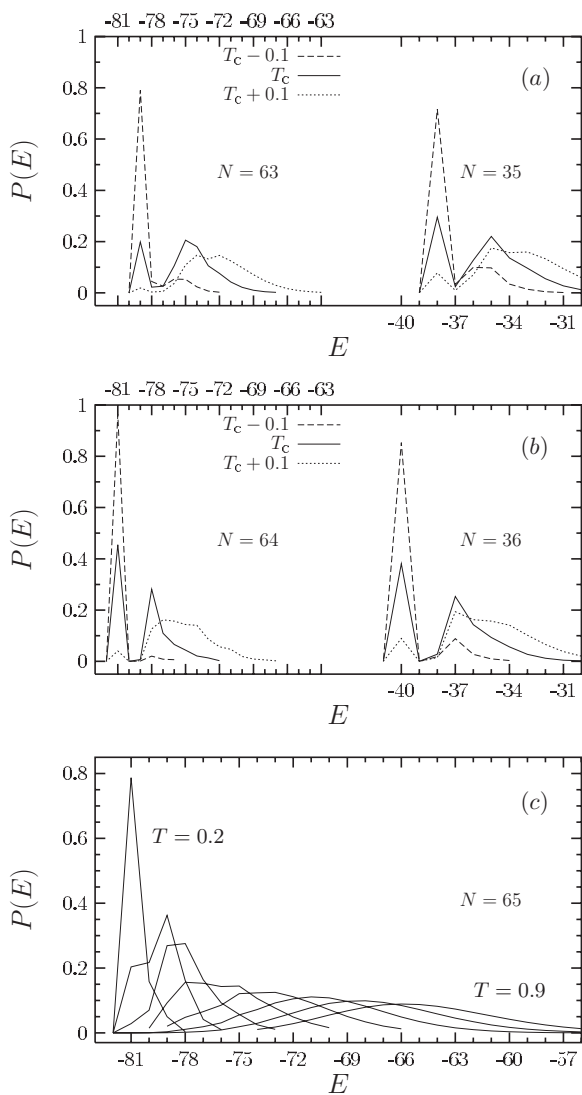
FIG. 6. Energy distributions $P(E)$ at low temperatures for sc lattice polymers with (a) $N=N_c-1=35$ and 63, (b) $N=N_c=36$ and 64 monomers. In (c), $P(E)$ is shown for the chain with length $N=N_c+1=65$ for several temperatures $T=0.2,0.3,\ldots,0.9$. The distributions for $N=37$ (not shown) are similar. Note that lines are only guides to the eyes.

$\sqrt{2}$ (in units of the lattice constant). This is not surprising, as these conformations are tightly packed which ensures a maximum number of nearest-neighbor contacts and, therefore, lowest conformational energy. An obvious example is the ground-state conformation of the 13-mer as shown in Fig. 8(a) which corresponds to the intuitive guess for the most closely packed structure on an fcc lattice: a monomer with its 12 nearest neighbors ("3-7-3" layer structure). A simple contact counting yields 36 nearest-neighbor contacts which, by subtracting the $N-1=12$ covalent (nonenergetic) bonds, is equivalent to an energy $E=-24$. However, this lowest-energy conformation is degenerate. There is another conformation (not shown) consisting of only two "layers," one containing six (a triangle) and the other seven (a hexagon) monomers ("6-7" structure), with the same number of contacts.

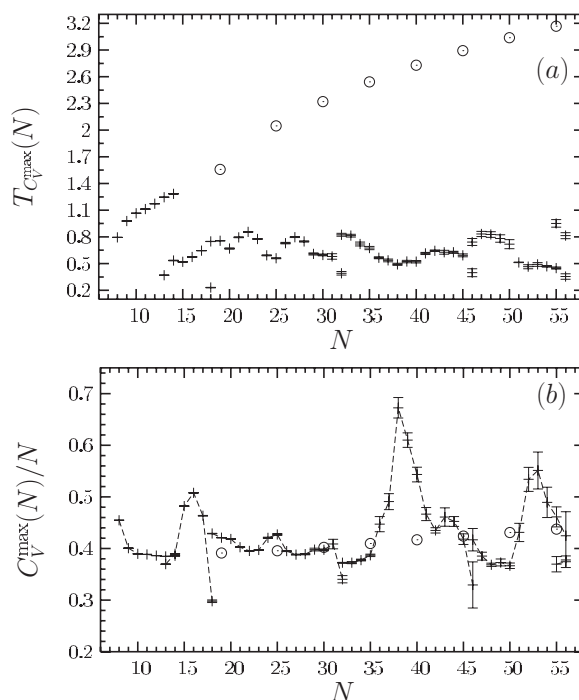FIG. 7. (a) Peak temperatures and (b) peak values of the specific heat for all chain lengths $N=8,\ldots,56$ of polymers on the fcc lattice. Circles ($\odot$) symbolize the collapse peaks and low-temperature peaks (+) signalize the excitation-freezing transitions. The error bars for the collapse transition are typically much smaller than the symbol size. Only for the freezing transition of longer chains, the statistical uncertainties are a little bit larger and visible in the plots. Θ peaks appear starting from $N=19$. For clarity, Θ data points are only shown for $N=19,25,30,\ldots$.

A special case is the 18-mer. As Fig. 8(b) shows, its ground state is formed by a complete triangle with six monomers, a hexagon in the intermediate layer with seven monomers, and an incomplete triangle (possessing a "hole" at a corner) with five monomers ("6-7-5" structure). Although this imperfection seems to destroy all rotational symmetries,
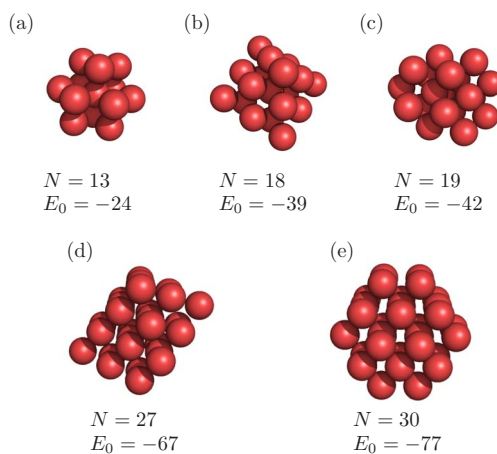

FIG. 8. (Color online) Ground-state conformations and energies of the (a) 13-, (b) 18-, (c) 19-, (d) 27-, and (e) 30-mer on the fcc lattice (bonds not shown).

it is compensated by an additional symmetry: Exchanging any of the triangle corners with the hole does not change the conformation at all. Thus, the seeming imperfection has a similar effect as the energetic excitation and causes a trivial entropic transition. This explains, at least partly, why the 18-mer exclusively exhibits an additional peak in the specific heat at very low temperatures [see Fig. 7(a)]. A similar reasoning presumably also applies to the anomalous low-temperature peaks of the 32-, 46-, and 56-mers, but for these larger ground-state conformations it does not make much sense to go into such intricate details.

The expectation that the 19-mer, which can form a perfect shape without any "holes" ("6-7-6" structure), is a prototype of peculiar behavior is, however, wrong. This is due to the existence of degenerate less symmetric ground-state conformations [as the exemplified conformation in Fig. 8(c)].

The described geometric peculiarities are, however, only properties of very short chains. One of the largest of the "small" chains that still possesses a nonspherical ground state, is the 27-mer with the ground-state conformation shown in Fig. 8(d). For larger systems, the relative importance of the interior monomers will increase, because of the larger number of possible contacts. This requires the number of surface monomers to be as small as possible which results in compact, spherelike shapes. A representative example is the 30-mer shown in Fig. 8(e).

D. The Θ transition revisited

The scaling behavior of several quantities at and close to the Θ point in three dimensions has been the subject of a large number of field-theoretic and computational studies [8,11,16–18,20–26]. Nonetheless, the somewhat annoying result is that the nature of this phase transition is not yet completely understood. The associated tricritical $\lim_{n\to 0} O(n)$ field theory has an upper critical dimension $d_c=3$, but the predicted logarithmic corrections [4–6] could not yet be clearly confirmed from the numerical data produced so far. In our study of freezing and collapse on regular lattices, we mainly focused on the critical temperature T_Θ for polymers on the sc and on the fcc lattice. The sc value of T_Θ has already been precisely estimated in several studies, but only a few values are known for the fcc case. Some previous estimates in the literature are compiled in Table I.

As our main interest is devoted to the expected difference of the collapse and freezing temperatures, we will focus here on the scaling behavior of the finite-size deviation of the maximum specific-heat temperature of a finite-length polymer from the Θ temperature, $T_c(N)-T_\Theta$, as it has also been studied for the bond-fluctuation model [12,13] and the off-lattice FENE polymer [14], as well as for polymer solution models [15,17,18]. In the latter case, Flory-Huggins mean-field theory [46] suggests

$$\frac{1}{T_{\text{crit}}(N)} - \frac{1}{T_\Theta} \sim \frac{1}{\sqrt{N}} + \frac{1}{2N}, \tag{3}$$

where $T_{\text{crit}}(N)$ is the critical temperature of a solution of chains of finite length N and $T_\Theta=\lim_{N\to\infty} T_{\text{crit}}(N)$ is the collapse transition temperature. In this case, field theory [4] pre-

TABLE I. T_Θ values on the sc and fcc lattice from literature.

Lattice type	T_Θ	Model	Reference
sc	3.64–4.13	Single chain	[20]
	3.713±0.007	Single chain	[21]
	3.650±0.08	Single chain	[23]
	3.716±0.007	Single chain	[8]
	3.60±0.05[a]	Single chain	[9]
	3.62±0.08[b]	Single chain	[10]
	3.717±0.003	Single chain	[11]
	3.717±0.002	Polymer solution	[16]
	3.745	Lattice theory	[25]
	3.71±0.01	Polymer solution	[17,18]
fcc	8.06–9.43	Single chain	[20]
	8.20±0.02	Single chain	[22,24]
	8.264	Lattice theory	[25]

[a]In Ref. [9] given as $\beta_\Theta=0.2779\pm0.0041$.
[b]In Ref. [10] given as $\beta_\Theta=0.276\pm0.006$.

dicts a multiplicative logarithmic correction of the form $T_{\text{crit}}(N)-T_\Theta \sim N^{-1/2}(\ln N)^{-3/11}$. Logarithmic corrections to the mean-field theory of single chains are known, for example, for the finite-chain Boyle temperature $T_B(N)$, where the second virial coefficient vanishes. The scaling of the deviation of $T_B(N)$ from T_Θ reads as [8]

$$T_B(N) - T_\Theta \sim \frac{1}{\sqrt{N}(\ln N)^{7/11}}. \tag{4}$$

In Ref. [14], it is claimed that, for their data obtained from simulations with the FENE potential, this expression can also be used as a fit ansatz for $T_c(N)-T_\Theta$. However, also the mean-field-motivated fit without explicit logarithmic corrections,

$$T_c(N) - T_\Theta = \frac{a_1}{\sqrt{N}} + \frac{a_2}{N}, \tag{5}$$

has been found to be consistent with the off-lattice data [14], and also with the results obtained by means of the bond-fluctuation model of single chains with up to 512 monomers [12,13]. Up to corrections of order $N^{-3/2}$, Eq. (5) is equivalent to

$$\frac{1}{T_c(N)} - \frac{1}{T_\Theta} = \frac{\tilde{a}_1}{\sqrt{N}} + \frac{\tilde{a}_2}{N}, \tag{6}$$

which was found to be consistent with numerical data obtained in grand canonical analyses of lattice homopolymers and the bond-fluctuation model [15,17,18].

The situation remains diffuse as there is still no striking evidence for the predicted logarithmic corrections (i.e., for the field-theoretical tricritical interpretation of the Θ point) from experimental or numerical data. Using our data from independent long-chain nPERMss [28] chain-growth simulations (sc, $N_{\max}=32\,000$; fcc, $N_{\max}=4000$) in the vicinity of the collapse transition, we have performed a scaling analysis of the N-dependent collapse transition temperatures $T_c(N)$,
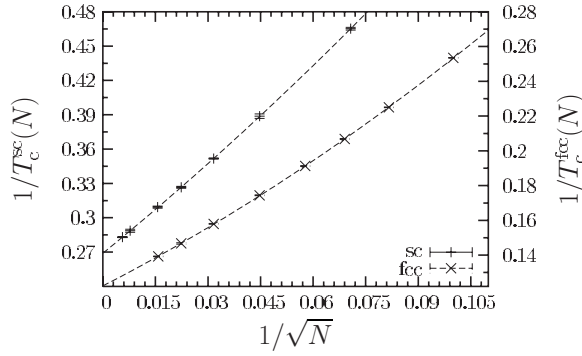
FIG. 9. Inverse collapse temperatures for several chain lengths on sc ($N \leq 32\,000$) and fcc lattices ($N \leq 4000$). Drawn lines are fits according to Eq. (6).

identified as the collapse peak temperatures of the individual specific-heat curves, and estimated from it the $N \rightarrow \infty$ limit T_Θ. For the single-chain system, field theory [5] predicts the specific heat to scale at the Θ point as $C_V(T=T_\Theta)/N \sim (\ln N)^{3/11}$. Short-chain simulations [23] did not reveal a logarithmic behavior at all, whereas for long chains a scaling closer to $\ln N$ was read off [11]. The situation is similar for structural quantities such as the end-to-end distance and the gyration radius. Figure 9 shows our data points of the inverse collapse temperature T_c^{-1} from the simulations on the sc (left-hand scale) and on the fcc lattice (right-hand scale), plotted

against $N^{-1/2}$. Error bars for the individual data points in Fig. 9 were obtained by jackknife error estimation [47] from several independent simulation runs. Also shown are respective fits according to the ansatz (6). Optimal fit parameters using the data in the intervals $200 \leq N \leq 32\,000$ (sc) and $100 \leq N \leq 4000$ (fcc) were found to be $T_\Theta^{sc}=3.72(1)$, $\tilde{a}_1 \approx 2.5$, and $\tilde{a}_2 \approx 8.0$ (sc) and $T_\Theta^{fcc}=8.18(2)$, $\tilde{a}_1 \approx 1.0$, and $\tilde{a}_2 \approx 5.5$ (fcc). In addition, we investigated also other fit functions motivated by field theory and mean-field-like approaches, corresponding to Eqs. (3)–(6), each of which also with different fit ranges. These results are listed in Tables II and III, respectively. In order to decide which of the fits is consistent with our data, the χ^2 test is used. Depending on the sizes of the data sets entering into the analyses and the number of fit parameters, there are 2 to 6 degrees of freedom d_f. We make the typical assumption that deviations of the fit from the used data set are significant, if $\chi^2 > \chi^2_{d_f;0.05}$, i.e., if χ^2 lies in the 5% tail of the $p_{d_f}(\chi^2)$ distribution of χ^2 values. In this case, with 95% probability the deviations between data and fit function are not random. The thresholds for the different degrees of freedom lie between $\chi^2_{2;0.05}/d_f=3.0$ and $\chi^2_{6;0.05}/d_f=2.1$. The calculated χ^2 values associated with the data sets and the fit functions used are also listed in Tables II and III.

From the results in Table II for the polymers on the sc lattice, we find that the two-parameter mean-field-like fits (5) and (6) as well as the single-parameter fit according to (3) are consistent with our data. Surprisingly poor, on the other

TABLE II. Values of T_Θ on the sc lattice from different fits and their χ^2 tests with several degrees of freedom d_f.

Fit function	T_Θ	a, respectively, a_1, a_2	N	χ^2/d_f	d_f
$T_c(N)-T_\Theta=a/\sqrt{N}$	3.6671 ± 0.0051	-26.0	500–32 000	12.7	4
	3.6741 ± 0.0053	-26.5	1000–32 000	6.61	3
	3.6898 ± 0.0065	-28.3	2000–32 000	1.39	2
$T_c(N)-T_\Theta=a(\ln N)^{7/11}/\sqrt{N}$	3.7353 ± 0.0056	-8.24	500–32 000	0.57	4
	3.7370 ± 0.0057	-8.27	1000–32 000	0.21	3
	3.7398 ± 0.0072	-8.36	2000–32 000	0.10	2
$T_c(N)-T_\Theta=a/\sqrt{N}(\ln N)^{7/11}$	3.6164 ± 0.0048	-83.0	500–32 000	39.5	4
	3.6287 ± 0.0049	-86.0	1000–32 000	20.7	3
	3.6531 ± 0.0059	-97.6	2000–32 000	4.14	2
$1/T_c(N)-1/T_\Theta=a(1/\sqrt{N}+1/2N)$	3.7255 ± 0.0060	2.6	500–32 000	0.28	4
	3.7245 ± 0.0061	2.6	1000–32 000	0.11	3
	3.7221 ± 0.0076	2.6	2000–32 000	0.03	2
$1/T_c(N)-1/T_\Theta=a_1/\sqrt{N}+a_2/2N$	3.7173 ± 0.0071	$2.5, 8.0$	200–32 000	0.05	4
	3.7173 ± 0.0104	$2.5, 8.0$	500–32 000	0.07	3
	3.7194 ± 0.0131	$2.5, 6.3$	1000–32 000	0.07	2
$T_c(N)-T_\Theta=a_1/\sqrt{N}+a_2/N$	3.7030 ± 0.0059	$-32, 135$	200–32 000	0.53	4
	3.7090 ± 0.0078	$-32, 161$	500–32 000	0.25	3
	3.7140 ± 0.0104	$-33, 186$	1000–32 000	0.12	2

TABLE III. Values of T_Θ on the fcc lattice using the same methodology as in Table II for the sc lattice.

Fit function	T_Θ	a, respectively, a_1, a_2	N	χ^2/d_f	d_f
$T_c(N)-T_\Theta=a/\sqrt{N}$	7.2673 ± 0.0052	-34.1	100–4000	1000	6
	7.5760 ± 0.0070	-39.4	150–4000	418	5
	7.7101 ± 0.0080	-42.0	210–4000	213	4
	7.8445 ± 0.0096	-45.5	300–4000	67.8	3
	7.9561 ± 0.0013	-50.0	500–4000	13.6	2
$T_c(N)-T_\Theta=a(\ln N)^{7/11}/\sqrt{N}$	7.9218 ± 0.0064	-15.2	100–4000	200	6
	8.0757 ± 0.0083	-16.1	150–4000	69.2	5
	8.1356 ± 0.0093	-16.5	210–4000	32.7	4
	8.1953 ± 0.0110	-17.0	300–4000	9.45	3
	8.2468 ± 0.0149	-17.6	500–4000	1.00	2
$T_c(N)-T_\Theta=a/\sqrt{N}(\ln N)^{7/11}$	6.8260 ± 0.0045	-79.5	100–4000	2000	6
	7.2258 ± 0.0062	-99.3	150–4000	1000	5
	7.4166 ± 0.0072	-110.2	210–4000	500	4
	7.6051 ± 0.0087	-125.7	300–4000	164	3
	7.7544 ± 0.0011	-146.3	500–4000	38.1	2
$1/T_c(N)-1/T_\Theta=a(1/\sqrt{N}+1/2N)$	8.5434 ± 0.0110	1.27	100–4000	111	6
	8.4208 ± 0.0120	1.23	150–4000	29.6	5
	8.3821 ± 0.0125	1.22	210–4000	13.5	4
	8.3369 ± 0.0141	1.20	300–4000	3.00	3
	8.3048 ± 0.0187	1.18	500–4000	1.15	2
$1/T_c(N)-1/T_\Theta=a_1/\sqrt{N}+a_2/2N$	8.1778 ± 0.0169	$1.04, 5.49$	100–4000	0.81	5
	8.1987 ± 0.0211	$1.06, 5.04$	150–4000	0.32	4
	8.2107 ± 0.0259	$1.07, 4.75$	210–4000	0.21	3
	8.2288 ± 0.0386	$1.09, 4.18$	300–4000	0.11	2
$T_c(N)-T_\Theta=a_1/\sqrt{N}+a_2/N$	8.0374 ± 0.0110	$-58.9, 360$	100–4000	13.1	5
	8.0876 ± 0.0133	$-61.5, 414$	150–4000	4.71	4
	8.1219 ± 0.0163	$-63.5, 461$	210–4000	1.81	3
	8.1640 ± 0.0244	$-66.5, 541$	300–4000	0.04	2

hand, is the goodness of the fit against the logarithmic scaling (4). Even more astonishing is, however, the good coincidence with a logarithmic fit of the "wrong" form $N^{-1/2}(\ln N)^{7/11}$ with the data. Summarizing these results, if logarithmic corrections as predicted by tricritical field theory are present at all, even chain lengths $N=32\,000$ on an sc lattice are too small to observe deviations from the mean-field picture. At least, the goodness of the logarithmic fit with the "wrong" exponent $+7/11$ could lead to the speculative conclusion that for $N\le32\,000$ multiplicative and additive logarithmic corrections to scaling are hidden in the fit parameters of the "mean-field-like fits." The subleading additive corrections are expected to be of the form $\ln(\ln N)/\ln^2 N$ [7]. They thus not only disappear very slowly—they are also even of the same size as the leading scaling behavior, which makes it extremely unlikely to observe the logarithmic corrections in computational studies at all [7]. Similar additive logarithmic scaling is also known, for example, from studies of the two-dimensional *XY* spin model [48]. The estimated sc Θ temperatures from the good fits are in perfect agreement with the most reliable estimates from literature.

The corresponding fcc results are listed in Table III. In this case, only the fit function (6) is independent of the data ranges used and, therefore, consistent with the data obtained for all chain lengths. However, the noticeable improvement of the goodness for the fits to (5) and (3), and the "wrong" $N^{-1/2}(\ln N)^{7/11}$ form by excluding the very short chains from the data sets considered, leads to the conclusion that even chains with $N=4000$ monomers on the fcc lattice are also too short to find evidence for the logarithmic corrections to mean-field scaling. Our best estimates for the fcc Θ temperature agree nicely with the results from Refs. [22,24].

IV. SUMMARY

Employing sophisticated chain-growth algorithms, we have performed computer simulations of homopolymers on

sc and fcc lattices in order to analyze freezing and collapse of these chains. Particular attention has been devoted to the question whether these transitions fall together in the thermodynamic limit as it was reported recently from similar studies of a specific bond-fluctuation model. In our analysis, we focus on the shifts of the specific-heat peaks in dependence of the chain-lengths considered.

For polymers on the sc lattice, we find a remarkably systematic pattern of the freezing transition which can be explained by lattice effects of the finite-length systems. In fact, the high precision of our data allows us to reveal a noticeable difference in the behavior of "magic" chain lengths that allow for cubic or cuboid conformations. In these cases, an energy gap exists between the ground-state conformations and the first excitations. This peculiarity causes a first-order-like pseudotransition which is typically more pronounced than the separate freezing transition. Surprisingly, this effect vanishes widely for polymers with slightly longer chain lengths. The freezing temperature decreases with increasing chain length until the next "magic" length is reached. Polymers on the fcc lattice behave similarly, but the relevant geometries are more complex.

We have also performed comprising analyses of the collapse temperature deviations for finite-length polymers from the Θ temperature, i.e., the collapse transition temperature in the limit of infinite chain length. We studied chains with lengths of up to 32 000 (sc) and 4000 (fcc) monomers, respectively. The thus obtained data were fitted against several fit functions motivated by field-theoretic and mean-field-like approaches. For the chain lengths studied, we find no evidence for logarithmic corrections as predicted by tricritical field theory. We conclude that the chain lengths are still too short to uniquely identify logarithmic corrections which are probably effectively taken into account by the amplitudes of the dominant mean-field terms.

From our results for the freezing and the collapse transition, we conclude that both transitions remain well separated also in the extrapolation toward the thermodynamic limit. This is the expected behavior as it is a consequence of the extremely short range of attraction in the nearest-neighbor lattice models used. Considering a more general square-well contact potential between nonbonded monomers in our parametrization,

$$v(r) = \begin{cases} \infty, & r \leq 1, \\ -1, & 1 < r \leq \lambda, \\ 0, & \lambda < r, \end{cases} \tag{7}$$

the attractive interaction range is simply $R = \lambda - 1$. In our single-chain study of sc and fcc lattice models, we have

$\lambda \to 1$ and thus $R \to 0$. Since this R value is well below a crossover threshold known for colloids interacting via Lennard-Jones-like and Yukawa potentials, where different solid phases can coexist, $R_c^{(1)} \approx 0.01$ [49–51], we interpret our low-temperature transition as the restructuring or "freezing" of compact globular shapes into the (widely amorphous) polymer crystals.

Following Ref. [52], there is also *another* phase boundary, namely between stable and metastable colloidal vapor-liquid (or coil-globule) transitions, in the range $0.13 < R_c^{(2)} < 0.15$. Other theoretical and experimental approaches yield slightly larger values, $R_c^{(2)} \approx 0.25$ [49,53–55]. Below $R_c^{(2)}$, the liquid (globule) phase is only metastable. The specific bond-fluctuation model used in Ref. [12] corresponds to $R = 0.225$, i.e., it lies in the crossover regime between the stable and metastable liquid phase [13]. Consequently, the crystallization and collapse transition merge in the infinite-chain limit and a stable liquid phase was only found in a subsequent study of a bond-fluctuation model with larger interaction range [13].

Qualitatively, analogous to the behavior of colloids, our considerations would explain the separate stable crystal, globule, and random-coil (pseudo)phases that we have clearly identified in our lattice polymer study. Since the range of interactions seems to play a crucial, quantitative role, it is an interesting, still widely open question to what extent the colloidal picture in the compact crystalline and globular phases is systematically modified for polymers with different nonbonded interaction ranges, where steric constraints (through covalent bonds) are *a priori* not negligible.

[1] For the difficulty of characterizing the type of the coil-globule transition, see, e.g., the review by I. M. Lifshitz, A. Yu. Grosberg, and A. R. Kokhlov, Rev. Mod. Phys. **50**, 683 (1978).

[2] A. R. Khokhlov, Physica A **105**, 357 (1981).

[3] P.-G. de Gennes, *Scaling Concepts in Polymer Physics* (Cornell University Press, Ithaca, 1979).

[4] B. Duplantier, J. Phys. (France) **43**, 991 (1982); J. Chem. Phys. **86**, 4233 (1987).

[5] B. Duplantier, Europhys. Lett. **1**, 491 (1986).

[6] M. J. Stephen, Phys. Lett. **53A**, 363 (1975).

[7] J. Hager and L. Schäfer, Phys. Rev. E **60**, 2071 (1999).

[8] P. Grassberger and R. Hegger, J. Chem. Phys. **102**, 6881

(1995).

[9] M. C. Tesi, E. J. Janse van Rensburg, E. Orlandini, and S. G. Whittington, J. Phys. A **29**, 2451 (1996).

[10] M. C. Tesi, E. J. Janse van Rensburg, E. Orlandini, and S. G. Whittington, J. Stat. Phys. **82**, 155 (1996).

[11] P. Grassberger, Phys. Rev. E **56**, 3682 (1997).

[12] F. Rampf, W. Paul, and K. Binder, Europhys. Lett. **70**, 628 (2005).

[13] F. Rampf, W. Paul, and K. Binder, J. Polym. Sci., Part B: Polym. Phys. **44**, 2542 (2006).

[14] D. F. Parsons and D. R. M. Williams, J. Chem. Phys. **124**, 221103 (2006); Phys. Rev. E **74**, 041804 (2006).

[15] N. B. Wilding, M. Müller, and K. Binder, J. Chem. Phys. **105**, 802 (1996).

[16] H. Frauenkron and P. Grassberger, J. Chem. Phys. **107**, 9599 (1997).

[17] A. Z. Panagiotopoulos, V. Wong, and M. A. Floriano, Macromolecules **31**, 912 (1998).

[18] Q. Yan and J. J. de Pablo, J. Chem. Phys. **113**, 5954 (2000).

[19] M. A. Anisimov and J. V. Sengers, Mol. Phys. **103**, 3061 (2005).

[20] F. L. McCrackin, J. Mazur, and C. M. Guttman, Macromolecules **6**, 859 (1973).

[21] W. Bruns, Macromolecules **17**, 2826 (1984).

[22] J. Batoulis and K. Kremer, Europhys. Lett. **7**, 683 (1988).

[23] H. Meirovitch and H. A. Lim, J. Chem. Phys. **92**, 5144 (1990).

[24] K. Kremer, in *Monte Carlo and Molecular Dynamics of Condensed Matter Systems*, edited by K. Binder and G. Cicotti (Editrice Compositori, Bologna, 1996), p. 669.

[25] M. P. Taylor and J. E. G. Lipson, J. Chem. Phys. **109**, 7583 (1998).

[26] A. L. Owczarek and T. Prellberg, Europhys. Lett. **51**, 602 (2000).

[27] M. N. Rosenbluth and A. W. Rosenbluth, J. Chem. Phys. **23**, 356 (1955).

[28] H.-P. Hsu, V. Mehra, W. Nadler, and P. Grassberger, J. Chem. Phys. **118**, 444 (2003); Phys. Rev. E **68**, 021113 (2003).

[29] M. Bachmann and W. Janke, Phys. Rev. Lett. **91**, 208105 (2003); J. Chem. Phys. **120**, 6779 (2004).

[30] T. Prellberg and J. Krawczyk, Phys. Rev. Lett. **92**, 120602 (2004).

[31] M. Bachmann and W. Janke, Phys. Rev. Lett. **95**, 058102 (2005); Phys. Rev. E **73**, 041802 (2006).

[32] J. Krawczyk, T. Prellberg, A. L. Owczarek, and A. Rechnitzer, Europhys. Lett. **70**, 726 (2005).

[33] D. S. Gaunt and A. J. Guttmann, in *Phase Transitions and Critical Phenomena*, edited by C. Domb and M. S. Green (Academic, London, 1974), p. 181.

[34] J. L. Cardy and A. J. Guttmann, J. Phys. A **26**, 2485 (1993).

[35] D. MacDonald, D. L. Hunter, K. Kelly, and N. Jan, J. Phys. A **25**, 1429 (1992).

[36] S. Caracciolo, M. S. Causo, and A. Pelissetto, Phys. Rev. E **57**, R1215 (1998).

[37] R. Guida and J. Zinn-Justin, J. Phys. A **31**, 8103 (1998).

[38] D. MacDonald, S. Joseph, D. L. Hunter, L. L. Moseley, N. Jan, and A. J. Guttmann, J. Phys. A **33**, 5973 (2000).

[39] M. Chen and K. Y. Lin, J. Phys. A **35**, 1501 (2002).

[40] T. Vogel, Diploma thesis, Universität Leipzig, 2004.

[41] R. Schiemann, M. Bachmann, and W. Janke, J. Chem. Phys. **122**, 114705 (2005).

[42] D. Aldous and U. Vazirani, "Go with the winners' algorithms," in *Proceedings of the 35th Annual Symposium on Foundations of Computer Science, Santa Fe* (IEEE, Los Alamitos, 1994), p. 492.

[43] This gap is an artifact of the simple-cubic lattice and the resulting excitation transition is a noncooperative effect: Consider a cuboid conformation with a chain end located in one of the corners. It forms two energetic contacts with the nearest neighbors nonadjacent within the chain. Performing a local off-cube pivot rotation of the bond the chain end is connected with, these two contacts are lost and no new contact is formed.

[44] D. H. E. Gross, *Microcanonical Thermodynamics* (World Scientific, Singapore, 2001).

[45] C. Junghans, M. Bachmann, and W. Janke, Phys. Rev. Lett. **97**, 218103 (2006).

[46] P. J. Flory, *Principles of Polymer Chemistry* (Cornell University Press, Ithaca, 1953).

[47] R. G. Miller, Biometrika **61**, 1 (1974); B. Efron, *The Jackknife, the Bootstrap, and Other Resampling Plans* (SIAM, Philadelphia, 1982).

[48] W. Janke, Phys. Rev. B **55**, 3580 (1997).

[49] A. Daanoun, C. F. Tejero, and M. Baus, Phys. Rev. E **50**, 2913 (1994).

[50] P. Bolhuis and D. Frenkel, Phys. Rev. Lett. **72**, 2211 (1994).

[51] C. F. Tejero, A. Daanoun, H. N. W. Lekkerkerker, and M. Baus, Phys. Rev. Lett. **73**, 752 (1994).

[52] M. G. Noro and D. Frenkel, J. Chem. Phys. **113**, 2941 (2000).

[53] C. Rascón, G. Navascués, and L. Mederos, Phys. Rev. B **51**, 14899 (1995).

[54] S. M. Ilett, A. Orrock, W. C. K. Poon, and P. N. Pusey, Phys. Rev. E **51**, 1344 (1995).

[55] N. Asherie, A. Lomakin, and G. B. Benedek, Phys. Rev. Lett. **77**, 4832 (1996).